

Multi-Layered Control of a Four-Degree-of-Freedom Mobile Robot with Compliant Linkage

by

Johann Borenstein
The University of Michigan

Abstract

This paper introduces a new approach to the design and control of a four-degree-of-freedom (4DOF) vehicle. This vehicle can travel sideways and it can negotiate tight turns easily. Existing 4DOF vehicles have been found difficult to control because of their overconstrained nature. These difficulties translate into severe wheel slippage or jerky motion under certain driving conditions.

Our approach overcomes these difficulties by introducing compliant linkage, a new concept in the control and kinematic design of 4DOF mobile robots. As the name implies, compliant linkage provides compliance between the drive wheels or drive axles of a vehicle, to accommodate control errors which would otherwise cause wheel slippage. We describe a three-level control system comprising of a wheel-level, a vehicle-level, and a trajectory-level controller. Experimental results are presented and show that control errors are effectively absorbed by the compliant linkage, resulting in smooth and precise motion.

1. Introduction

Most conventional mobile robots use either a *differential drive* design (i.e., two drive wheels, each with its own motor [Pritschow et al, 1988]), or a *tricycle* design where one wheel is steered and driven [Hammond, G., 1986; Wiklund et al., 1988]. Such vehicles have two independently controlled axis and are easy to control. However, in many applications floor space is limited and vehicles with better maneuverability are needed. Superior maneuverability has been demonstrated with three-degree-of-freedom (3DOF) vehicles, which use specially designed roller-wheels that can move sideways [Leifer et al., 1988, Feng et al., 1989]. These vehicles, however, are subject to inaccuracies and don't function well on rough surfaces [Killough and Pin, 1992]. Another class of vehicles, collectively called *multi-degree-of-freedom* (MDOF) vehicles, allow complex motions through the use of 4 or more motors. Such vehicles are extremely maneuverable; they are capable of turning in confined space, moving sideways, and performing other maneuvers that would allow the vehicle to move along a mathematically optimal trajectory. The disadvantage of these vehicles is the difficulty of translating 4 (or more) DOF of control to the three DOF of motion that are possible in the plane (overconstrained systems). Typically, this translation requires to maintain an accurate relation between the momentary velocities of the wheels and the momentary kinematic configuration (Alexander and Maddocks, 1989). This relation can usually be expressed in a single equation, known as the "*rigid body constraint*." Any violation of the *rigid body constraint* — even temporarily — will cause wheel slippage, a highly undesirable effect in dead-reckoning mobile robots [Reister, 1991].

Realizing that it is practically impossible to implement speed controllers that guarantee accurate velocity matching at all times (especially during transients), we have overcome this problem by

introducing the concept of *compliant linkage*. The compliant linkage allows relative motion between wheels, thereby effectively removing the rigid body constraint.

2. The compliant linkage

As explained above, the key element in any workable MDOF design must be the provision of *mechanical compliance* [Borenstein, 1992]. One possible kinematic design for an MDOF vehicle is shown in Fig. 1.

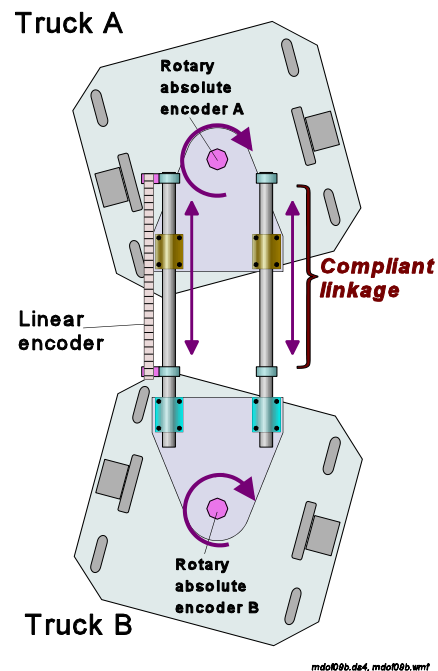


Figure 1: A dual-differential drive vehicle with compliant linkage.

This vehicle has two independent *chassis*' that are free to rotate about a vertical shaft connected to the vehicle body. Each chassis comprises of two drive motors, along with their respective reduction gears, encoders, and drive wheels. Each pair of drive wheels is located on a common axes and forms a *differential drive system* capable of moving forward, backward, and rotating — simply by controlling the velocities of the drive wheels. Each chassis also holds 4 castors, for stability when traveling sideways. We will call this vehicle, which combines two differential drive systems, a *dual differential drive* (DDD) vehicle. Mechanical compliance is implemented by means of a longitudinal slider, based on a linear bearing that allows relative motion between the front and rear chassis. Besides the encoders that are attached to each one of the drive motors, three additional encoders are used: one rotary encoder on each of the two vertical shafts, and one linear encoder on a longitudinal slider. Figure 2 shows our

experimental vehicle, which is 1.4 m long and 0.6 m wide. The individual chassis' are commercially available *LABMATE*[®] [TRC] platforms. On top of the vehicle, covering both chassis', is a plexiglass plate that provides a continuous, flat loading space.



Figure 2: The experimental dual differential drive vehicle, built and tested at the University of Michigan.

3. The control system

The control system is implemented on a 486-based IBM-AT compatible computer running at 33 MHz. The system comprises of three functional levels (Fig. 3) that are discussed below.

3.1 The chassis-level controller

At the lowest level of the controller hierarchy are two *chassis-level* controllers (see Fig. 4). The purpose of these controllers is to maintain the velocities of each drive wheel, according to reference velocities prescribed by the vehicle-level controller. The chassis level controllers have an inner velocity feedback loop, which uses the commercially available, programmable HCTL 1100 motion controller chip [Hewlett Packard]; one for each motor. These chips perform quadrature decoding of the incremental wheel encoder output, compute the actual velocity of the motors, V_m , and compare this velocity with the reference velocity V prescribed by the outer control loop. The difference $E = V_r - V_m$ is the error signal of the inner loop. Set-up to operate as P-type controllers, the chips then issue *pulse width modulation* (PWM) signals to the PWM amplifiers, in proportion to the computed error E . The inner loop performs at a sampling time of $T_i = 4$ ms. The outer loop of the chassis-level controllers is a modified implementation of the cross-coupled controller developed earlier by Borenstein and Koren [1987] for accurate control of differential drive mobile robots. The purpose of cross-coupling is to maintain an accurate ratio between the velocities of the two drive motors in a differential drive vehicle. The overall effect of the cross-coupled control is the elimination of the steady-state orientation error of a chassis.

3.2 The vehicle-level controller

The vehicle-level controller is the central element in the compliant linkage vehicle; its task is to minimize deviations Δl from the *nominal* link-length L (i.e., the length of the *compliant link* that connects the two chassis'). The link-length is a function

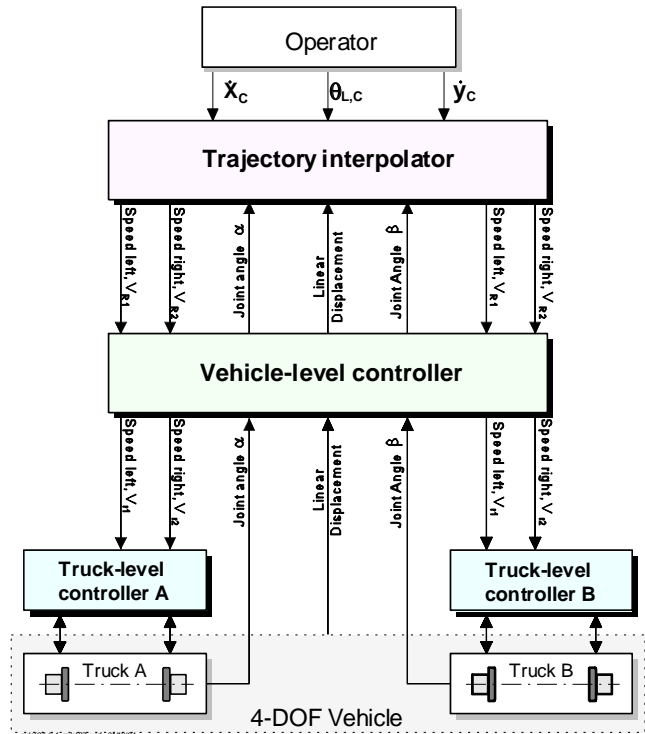


Figure 3: Components of the MDOF vehicle control system

of the speed of each chassis **and** its orientation relative to the link. This creates a difficulty that can be visualized by considering the two extreme case:

Case a: both chassis' are aligned longitudinally: In this case, the link-length can only be controlled by changing the translational speed of the chassis'.

Case b: both chassis' are facing 90° sideways: In this case, the *relative* speed is always zero, and the link-length can only be

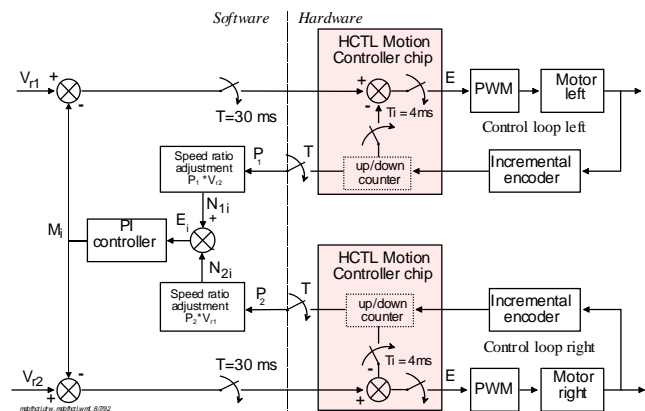


Figure 4: Chassis-level controller with modified cross-coupling and HCTL motion controller.

controlled by changing the orientation of the chassis'.

In actual operation one will encounter a combination of these two extreme cases. The resulting control problem is rather difficult; it requires control of the link-length by manipulating four motor velocities in a system where two basically different control laws must be superimposed (namely, cases a. and b., above) and where one of the control laws (case b.) is highly non-linear.

As a solution to this problem, we first define a simple *PI controller module*, to guarantee zero deviation from the nominal link-length under *steady state* conditions:

$$M_{PI} = K_P \Delta l + K_I \Sigma \Delta l \quad (1)$$

where

- M_{PI} — Output of the PI controller.
- K_P — Proportional gain of the PI controller.
- K_I — Integral gain of the PI controller.
- Δl — Deviation from the nominal link-length L .

For case (a) situations the *PI controller module* could be used as follows

$$V_{r,1} = V_{R,1}(1 - M_{PI}) \quad (2a)$$

$$V_{r,2} = V_{R,2}(1 - M_{PI}) \quad (2b)$$

$$V_{r,3} = V_{R,3}(1 + M_{PI}) \quad (2c)$$

$$V_{r,4} = V_{R,4}(1 + M_{PI}) \quad (2d)$$

where

- $V_{R,i}$ — Required reference speed as received from the trajectory level controller.
- $V_{r,i}$ — Modified reference speed, passed-on to the chassis-level controller.

The link-length controller described by Eqs. (2) works as follows: Suppose at some instance the leading chassis A is faster than the trailing chassis B. This situation would result in an increased link-length l , or a positive Δl , and consequently a positive M_{PI} . Equations (2) then modify the reference velocities such that the speed of the leading chassis is reduced, while the speed of the trailing chassis is increased.

This simple link-length controller works well only if the two chassis' are aligned longitudinally (i.e., α and β are small). If α or β are large, then modifying the speed of a chassis is less effective. During fully 90° sideways crabbing, this control is in fact totally ineffective. If no additional measures are taken, then a small deviation from the link-length can grow over time and cause the controller to induce large (but ineffective) changes in the velocities of the chassis', resulting in instable motion.

For this reason we introduce a further modification to the link-length controller. The modified controller applies a *rotational* correction (by increasing the difference between the velocities of the motors of a chassis) when α or β are large, while reducing the gain of the translational (i.e., the sum of the velocities of the motors on one chassis) component. Eqs. (3) shows how the modified controller is implemented.

$$V_{r,1} = V_{R,1} [1 + M_{PI} (-\cos\alpha - \sin\alpha)] \quad (3a)$$

$$V_{r,2} = V_{R,2} [1 + M_{PI} (-\cos\alpha + \sin\alpha)] \quad (3b)$$

$$V_{r,3} = V_{R,3} [1 + M_{PI} (+\cos\beta + \sin\beta)] \quad (3c)$$

$$V_{r,4} = V_{R,4} [1 + M_{PI} (+\cos\beta - \sin\beta)] \quad (3d)$$

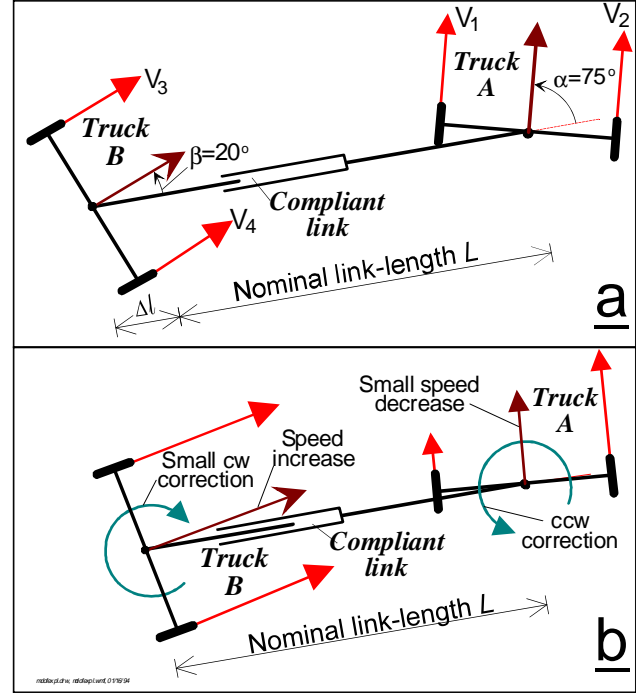


Figure 5:
Example for operation of vehicle-level controller.
a. Link-length is too large. b. After corrective action.

As an example, we consider a typical situation like the one shown in Fig. 5a, where $\alpha = 75^\circ$, $\beta = 20^\circ$, and $M_{PI} > 0$ (i.e., the compliant link is extended beyond its nominal length). Applying the modified controller of Eqs. (3), we note that $\cos\alpha$ is small, $\sin\alpha$ is large, and the sum of the two trigonometric terms in Eq. (3a) is negative. Consequently, $V_{r,1}$ will be reduced. Similarly, $V_{r,2}$ will be increased, since the dominant $\sin\alpha$ term has a positive sign. Thus, the absolute speed *difference* between the two drive wheels of the front chassis increases, modifying the motion prescribed by the *trajectory controller* (the highest level in the control hierarchy) such as to add a counter-clockwise rotational component, while slightly reducing the translational velocity of the chassis (see Fig. 5b). The counter-clockwise rotation orients the leading chassis more toward the trailing chassis, thereby reducing the relative speed between the two chassis and consequently the link-length. The effect of the controller on the trailing chassis can be examined in a similar way. In our example $\beta = 20^\circ$ is small, and therefore $\cos\beta$ is large. Since this term appears with a positive sign in Eqs. (3c) and (3d), it causes an increase in the translational velocity of the trailing chassis, as shown in Fig. 5b. Consequently, the trailing chassis can "catch up" with the leading chassis and the link length is reduced. Note that the $\sin\beta$ terms in Eqs. (3c) and (3d) have opposite signs, causing a clockwise rotation. A clockwise rotation helps align the trailing chassis with the compliant link, making the speed increase more effective although the rotational component is only small, since $\sin\beta$ is small.

3.3 The trajectory-level controller

The task of the *trajectory level controller* (TLC) is to generate reference velocity signals that direct the vehicle along a specific trajectory. The *trajectory level controller* described in this Section can be used to allow a human operator to control the vehicle motion with a 3-DOF joystick. Alternatively, a higher level path planner can send commands to the TLC, indicating a desired direction of travel. A direction is prescribed in terms of the x and y components of a directional vector, and a desired orientation. Operating in vehicle coordinates, a positive x-direction command will cause the vehicle to travel 90° sideways (crabbing to the right), and a positive y-direction command will cause straight forward travel. Our TLC features an *alignment* option, where the orientation input is used to specify an *absolute* orientation with which the vehicle attempts to align at all times.

We denote these high-level input commands to the *trajectory level controller* J_x , J_y , and J_θ , where J_x and J_y specify the components of the desired direction of travel, and J_θ is the desired absolute orientation.

For the discussion of the TLC it is convenient to define a new operator, which is called *angdist* and denoted $(-)$. $(-)$ is defined for two operands, γ_1 and γ_2 , and is used in the form $\delta = \gamma (-) \gamma_2$. The result, δ , is the shortest rotational distance between γ and γ_2 . Therefore, δ is always in the range $-180^\circ < \delta \leq 180^\circ$.

At first, the TLC uses the J_θ input to compute a reference angular velocity $\dot{\theta}_{L,ref}$ for the whole vehicle.

$$\dot{\theta}_{L,ref} = K_\theta \frac{\theta_L (-) J_\theta}{T} \quad (4)$$

where

- K_θ — Proportional gain factor for vehicle alignment.
- θ_L — Present vehicle orientation (defined as the orientation of the compliant link). This value is known initially and is then updated by dead-reckoning.
- T — Real-time sampling time (= 30 ms).

Next, the x and y velocity components for the desired motion of the two chassis' center points A and B are determined.

$$V_{Ay} = K_y J_y + \frac{1}{2} J \dot{\theta}_{L,ref} \quad (5)$$

$$V_{By} = K_y J_y - \frac{1}{2} J \dot{\theta}_{L,ref}$$

where

- V_{Ay} — Velocity y-component for the front chassis center point, in vehicle coordinates.
- V_{By} — Velocity y-component for the rear chassis center point, in vehicle coordinates.
- K_y — Proportional gain factor for y-direction input.

The J_x -input can be translated directly into the desired velocity components

$$V_{Ax} = K_x J_x \quad (6)$$

$$V_{Bx} = K_x J_x$$

where

- V_{Ax} — Velocity x-component for the front chassis center point, in vehicle coordinates.
- V_{Bx} — Velocity x-component for the rear chassis center point, in vehicle coordinates.
- K_x — Proportional gain factor for x-direction input.

Now, the TLC can compute the magnitude of the reference velocities for the front and rear chassis, $V_{A,ref}$ and $V_{B,ref}$.

$$V_{A,ref} = \sqrt{V_{Ax}^2 + V_{Ay}^2} \quad (7)$$

$$V_{B,ref} = \sqrt{V_{Bx}^2 + V_{By}^2}$$

The directions of the reference velocities for the front and rear chassis are

$$\alpha_{ref} = \arctan \frac{V_{Ax}}{V_{Ay}} \quad (8)$$

$$\beta_{ref} = \arctan \frac{V_{Bx}}{V_{By}}$$

In order to reach the desired reference directions α_{ref} and β_{ref} the front and rear chassis' have to rotate. This is accomplished by applying the following reference steering rates:

$$\dot{\alpha}_{ref} = K_c \frac{\alpha - \alpha_{ref}}{T} \quad (9)$$

$$\dot{\beta}_{ref} = K_c \frac{\beta - \beta_{ref}}{T}$$

where

- K_c — Proportional gain factor for steering.
- α — Relative angle between front chassis and link (measured by absolute encoder A).
- β — Relative angle between rear chassis and link (measured by absolute encoder B).
- $\dot{\alpha}_{ref}$ — Reference steering rate for front chassis.
- $\dot{\beta}_{ref}$ — Reference steering rate for rear chassis.

Some easily derived kinematic relations for the vehicle are

$$\dot{\theta}_A = \dot{\theta}_L + \dot{\alpha} \quad (10)$$

$$\dot{\theta}_B = \dot{\theta}_L + \dot{\beta} \quad (11)$$

where $\dot{\alpha}$ and $\dot{\beta}$ are derived from the absolute encoders, A and B, respectively, and $\dot{\theta}_A$ and $\dot{\theta}_B$ are the absolute steering rates of chassis A and B, respectively. Another generally valid kinematic relation for any given set of velocities V_A and V_B is

$$\begin{aligned}
V_1 &= V_A + \frac{b}{4\pi} \dot{\theta}_A \\
V_2 &= V_A - \frac{b}{4\pi} \dot{\theta}_A \\
V_3 &= V_B + \frac{b}{4\pi} \dot{\theta}_B \\
V_4 &= V_B - \frac{b}{4\pi} \dot{\theta}_B
\end{aligned} \tag{12}$$

Rewriting Eqs. (10) and (11) for the *reference* rotations, we have

$$\begin{aligned}
\dot{\theta}_{A,ref} &= \dot{\theta}_L + \dot{\alpha}_{ref} \\
\dot{\theta}_{B,ref} &= \dot{\theta}_L + \dot{\beta}_{ref}
\end{aligned} \tag{13}$$

Finally, rewriting Eqs. (12) specifically for the reference velocities $V_{A,ref}$ and $V_{B,ref}$ from Eq. (7) and substituting Eqs. (13) the reference velocities for all four drive wheels are obtained:

$$\begin{aligned}
V_{1,ref} &= V_A - \frac{b}{4\pi} \dot{\theta}_{A,ref} \\
V_{2,ref} &= V_A + \frac{b}{4\pi} \dot{\theta}_{A,ref} \\
V_{3,ref} &= V_B - \frac{b}{4\pi} \dot{\theta}_{B,ref} \\
V_{4,ref} &= V_B + \frac{b}{4\pi} \dot{\theta}_{B,ref}
\end{aligned} \tag{14}$$

The velocities on the left-hand side of Eqs. (14) are the reference signals that are sent to the *vehicle-level controller*.

4. Experimental results

The experiment described in this Section documents the function of the controller system, specifically of the vehicle-level controller. This controller aims at minimizing the *fluctuation* of the length of the *compliant link*, Δl : it is desirable that Δl remains small (relative to the vehicle size) since large fluctuations would be difficult to accommodate from an engineering point of view.

Figure 6a shows "snapshots" of the experimental vehicle during the execution of a preprogrammed motion-sequence. The trajectories of the center points of the front and rear chassis' are also plotted. Seven different motions (labeled "Action 1" through "Action 7" in Fig. 6a) were performed, and the location of the front chassis — at the moment a new action was invoked — is marked. The motions include forward and backward travel, rotation, and sideways crabbing, as well as the combination of these components. Furthermore, the whole sequence was performed fluently, without stopping between actions. The maximum speed was set to $V_{max} = 0.8$ m/s. However, the trajectory level controller reduces the maximum speed temporarily as a function of the rate of directional changes of the individual chassis'. Consequently, the average speed for the run was $V_{avg} = 0.42$ m/s.

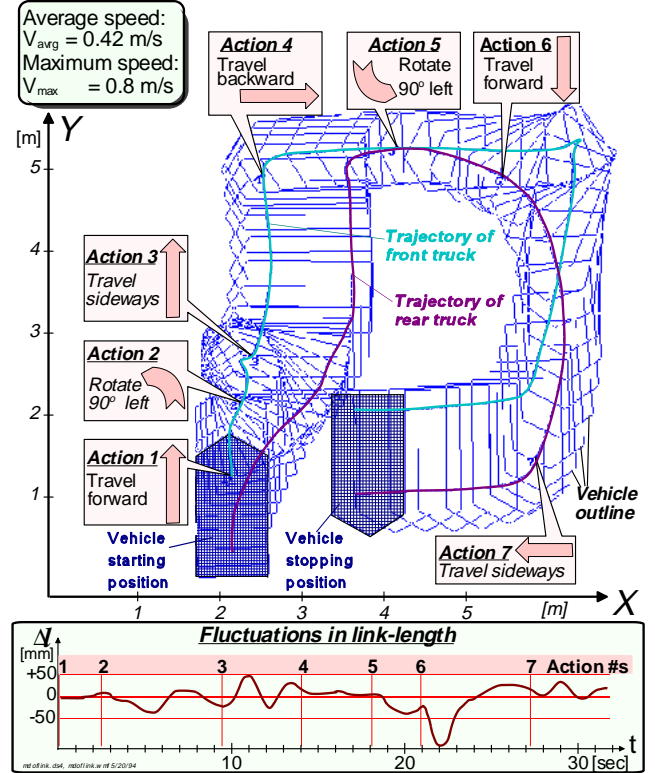


Figure 6: a. Trajectory of the 4-DOF vehicle after performing a multi-mode motion sequence. b. Fluctuations of link-length during the sequence of Fig. 6a.

Figure 6b shows the fluctuations in link-length during the run. The maximum deviation from the nominal link-length L was approximately $\Delta l = 12$ cm, and it occurred shortly after Action 6 was invoked. The compliant link shortened at this point because the rear chassis came to a complete halt to change direction (in the upper-right corner of Fig. 6a) while the front chassis was further approaching.

Recent experimental results reported in [Borenstein, 1993] show that the absolute motion accuracy are equal to that of conventional 2DOF mobile robots, even with extreme maneuvering.

5. Conclusions

We have introduced a new design for four-degree-of-freedom (4DOF) mobile robots. In this design a *compliant linkage* is used to accommodate temporary controller errors, which would otherwise violate the "rigid body constraint" and consequently cause wheel slippage.

The length of the compliant linkage must be controlled in order to avoid excessive fluctuations. Since this control makes use of the same actuators that are used to control direction and speed of the vehicle, we have developed an intermediate level of control, called *vehicle level controller*. This controller modifies reference velocities from the higher level, and passes them on to the lower level.

An experimental vehicle was built and extensively tested. The multi-level control system was found to provide smooth and stable motion at speeds of up to 0.5 m/s — even under vigorous joystick control. We believe that much higher speeds are feasible with more adequately designed drive chassis' (in our experimental vehicle we used off-the-shelf platforms, each with two heavy 12-Volt batteries onboard, which dramatically limited the responsiveness of the chassis to steering commands).

This research was funded by NSF grant # DDM-9114394 and by the Department of Energy.

6. Bibliography

1. Alexander, J.C. and Maddocks, J.H., 1989, "On the Kinematics of Wheeled Mobile Robots." *Int. Journal of Robotics Research*, Vol. 8, No. 5, August, pp. 15-27.
2. Borenstein, J. and Koren, Y., 1987, "Motion Control Analysis of a Mobile Robot." *Transactions of ASME, Journal of Dynamics, Measurement and Control*, v. 109, no .2, pp.73-79.
3. Borenstein, J., 1992, "Compliant-linkage Kinematic Design for Multi-degree-of-freedom Mobile Robots ." *Proceedings of the SPIE Symposium on Advances in Intelligent Systems, Mobile Robots VII*, Boston, MA, Nov. 15-20,
4. Borenstein, J., 1993, "Control and Kinematic Design for Multi-degree-of-freedom Mobile Robots With Compliant Linkage." Submitted for publication in the *IEEE Transactions on Robotics and Automation*, November 1992.
5. Feng, D., Friedman, M. B., and Krogh, B. H., 1989, "The Servo-Control System for an Omnidirectional Mobile Robot." *Proceedings of the 1989 IEEE International Conference on Robotics and Automation*, Scottsdale, Arizona, May 14-19, pp. 1566-1571.
6. Hammond, G., 1986, "AGVs at work: Automated Guided Vehicle Systems" Bedford, New York.
7. Hewlett Packard, "Optoelectronics Designer's Catalog, 91-92."
8. Killough, S. M. and Pin, F. G., 1992, "Design of an Omnidirectional Holonomic Wheeled Platform Prototype." *Proceedings of the IEEE Conference on Robotics and Automation*, Nice, France, May, pp. 84-90.
9. Leifer, L.J., Van der Loos, H.F. Chalowski, S.J., 1988, "Development of an Omni-directional Mobile Vocational Assistant Robot," *Proceedings of the International Conference of the Association for the Advancement of Rehabilitation Technology*, Montreal, Canada.
10. Pritschow, G., Jantzer, M., and Schumacher, H., 1988, "A Control System for Free-ranging Mobile Robots In Production Lines." *Proceedings of the 6th International Conference on Automated Guided Vehicle Systems 1988*, Brussels, Belgium, 25-26 October, pp. 189-197.
11. Reister, D. B., 1991, "A New Wheel Control System for the Omnidirectional HERMIES-III Robot." *Proceedings of the IEEE Conference on Robotics and Automation*, Sacramento, California, April 7-12.
12. Transition Research Corporation (TRC), 15 Great Pasture Road, Danbury, Connecticut 06810.
13. Wiklund et al., 1988, "AGV Navigation by Angle Measurement." *Proceedings of the 6th International Conference on Automated Guided Vehicle Systems 1988*, Brussels, Belgium, 25-26 October, pp. 199-212.